

**Synergistic effect of exfoliation and substitutional doping in graphitic carbon
nitride for photocatalytic H₂O₂ production and H₂ generation: A
Comparison and Kinetic Study**

Bhagyashree Priyadarshini Mishra, Lopamudra Acharya, and Kulamani Parida*

*Centre for Nano Science and Nano Technology, Institute of Technical Education and
Research, Siksha 'O' Anusandhan University, Bhubaneswar-751030*

**Corresponding author*

***Corresponding Author's Email:**

kulamaniparida@soa.ac.in

paridakulamani@yahoo.com

Tel. No.: +91-674-2351777 and Fax. +91-674-2350642

1. Materials

Melamine (99%), ammonium dihydrogen phosphate (99.9%), thiourea (99%), boric acid (99%), hydrochloric acid (36.5-38%), ethanol (99.9%), and methanol (99%) were purchased from Merck and were taken as precursors. All the above taken chemicals were used without any additional purification. Throughout the reaction, deionized water was used which has been collected from Millipore system.

2. Characterization: -

2.1 Physical characterizations:

To investigate the crystallographic structure and phase purity of the synthesized sample X ray diffraction (XRD) pattern was collected on a Rigaku Miniflex Ultima IV with Cu K α radiation (power rating: 100mA, 40kV and $\lambda=1.54\text{\AA}$). Fourier transform infrared spectroscopy (FTIR) measurement was used to give a more complete characterization of the surface structure. FTIR spectra were obtained with a frequency range between 400 to 4000 cm^{-1} using a JASCO-FT-IR-4600 spectrometer (with KBr as a reference). The morphological analysis of the as-synthesized photocatalysts was carried out by using FEG-SEM JSM-7600F for FESEM and HR-TEM 300 kV of model Tecnai G2, F30 for HRTEM study. UV-Vis diffuse reflectance spectroscopy was obtained using a JASCO-V-750 UV-visible spectrophotometer. Photoluminescence (PL) spectroscopy was used to evaluate the recombination rate and separation efficiency of plain and composite materials at ambient temperature using a JASCO FP-8300 spectrofluorometer with an excitation wavelength of 350 nm. The surface chemistry and elemental composition of the photocatalysts were examined by XPS using a Kartos axis ultra-x-ray photoelectron spectrometer, which was equipped with a monochromatized x-ray source (Al K α). The C 1s peak was considered as the reference peak.

2.2 Photoelectrochemical experiments:

Photoelectrochemical measurements, using a IVIUMSTAT multichannel workstation was performed where a conventional three electrode Pyrex cell with Pt and Ag/AgCl respectively as counter and reference electrode. For fabrication of working electrodes, an electrophoretic deposition method has been employed in which photocatalysts were deposited on Fluorine doped tin oxide (FTO). Typically to a beaker, 20 mg of photocatalyst and iodine were taken along with 20 mL of acetone, and the solution was dispersed properly by 10 min of sonication. In the above well-dispersed solution two parallel FTOs (separated by 10-15 mm) were dipped, and under controlled potentiostatic condition, 60 V bias was subjected (3 min) to coat the FTO

surface by the photocatalyst as a thin film in 1 cm² area. The photocatalyst deposited FTOs were kept for calcination in presence of air at 200^oC for 2 h so as to remove impurities from the FTO surface. Linear sweep voltammetry (LSV) was executed at scan rate of 25 mV/s applying potential of -2 to +2 V. Electrochemical impedance spectroscopy was also performed at zero biased potential at frequency 10⁻² to 10⁵ Hz. In dark condition, also the Mott-Schottky analysis was carried out. All the above electrochemical analysis were carried out using 0.1 M Na₂SO₄ solution and 0.1 M KOH solution as electrolyte.

3. Photocatalytic applications:

The photocatalytic activities of as-synthesized nanomaterials CN, e-PCN, e-SCN, and e-BCN were confirmed by (i) photocatalytic hydrogen evolution and (ii) photocatalytic H₂O₂ generation.

3.1 Photocatalytic H₂O₂ production experiment:

In an O₂-saturated environment, photocatalytic H₂O₂ generation was carried out using pristine CN, e-PCN, e-SCN, and e-BCN photocatalysts. For thorough dispersion, 0.02 g of photocatalysts were ultrasonicated for 10 minutes in a mixed solution of 19 mL DI water and 1 mL ethanol. Afterward the sample was bubbled with O₂ gas for 30 min to achieve O₂ equilibrated environment followed by irradiation with 250 W Xe lamp. After 2h of light illumination the photocatalysts were separated from the solution through centrifugation and filtration. Then 1 mL of resultant solution was mixed with 2 mL of KI (0.1 M) solution followed by the addition of 0.05 mL of ammonium molybdate (0.01 M) solution to accomplish a light-yellow colour. After the addition, the concentration of the H₂O₂ was measured by a UV-Vis spectrophotometer at a wavelength of 350 nm.

3.2 Photocatalytic Water Splitting Experiment for Hydrogen Evolution Reaction:

The catalytic efficiency of the fabricated nanomaterials were evaluated through photocatalytic water redox reaction under visible light using different scavengers. Photocatalytic water splitting experiment was performed in a sealed quartz batch reactor (100 mL capacity) fitted with 150 W Xe lamp (using cut off filter; 420 nm). A suspension was prepared by taking 20 mg catalyst in 10 % methanol (for H₂ evolution) solution under constant stirring. Here, 10 % methanol is used to scavenge holes from the semiconductor surface thereby providing electrons for water reduction, respectively. Nitrogen gas was purged into the solution for several minutes before irradiation to remove the dissolved gases and constant stirring was maintained to achieve proper dispersion of photocatalyst during the course of reaction. The photocatalytic reaction was performed at normal environmental condition with constant cold-water circulation, and the evolved gas was collected by downward displacement of water. Then, the gas was analysed

by a gas chromatograph (Agilent Technology) with molecular sieve (5 Å) column with a thermal conductive detector and the evolved gas was characterised to be hydrogen.

Equation S1. Triexponential function for TRPL fitting:

$$\text{Fit} = A + \alpha_1 \exp\{-t / \tau_1\} + \alpha_2 \exp\{-t / \tau_2\} + \alpha_3 \exp\{-t / \tau_3\}$$

Where A is a constant, α_1 , α_2 and α_3 are relative contributions and τ_1 , τ_2 and τ_3 are the decay lifetimes of the respective compounds. The average lifetimes (τ_{avg}) of e-PCN, e-SCN, and e-BCN were determined by using equation below:

$$\tau_{\text{avg}} = \frac{\alpha_1 \tau_1^2 + \alpha_2 \tau_2^2 + \alpha_3 \tau_3^2}{\alpha_1 \tau_1 + \alpha_2 \tau_2 + \alpha_3 \tau_3} \dots\dots\dots(1)$$

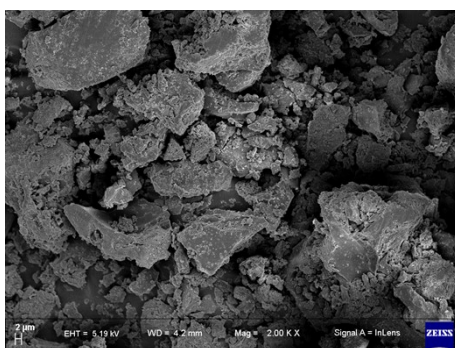


Figure S1 FESEM image of pristine CN.

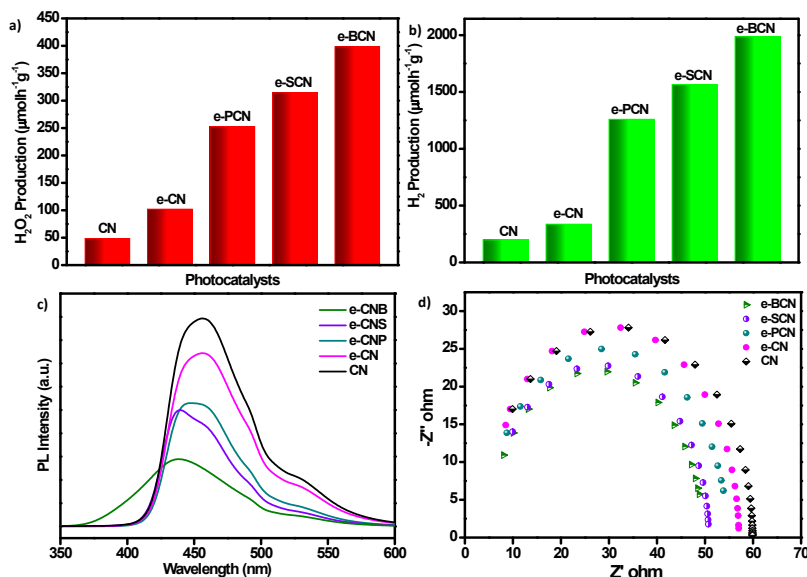


Figure S2 a) Photocatalytic H₂O₂ production after 2 h irradiation, b) Photocatalytic H₂ evolution by CN, e-CN, e-PCN, e-SCN, and e-BCN photocatalysts, c) photoluminescence spectra d) EIS spectra of CN, e-CN, e-PCN, e-SCN, and e-BCN.

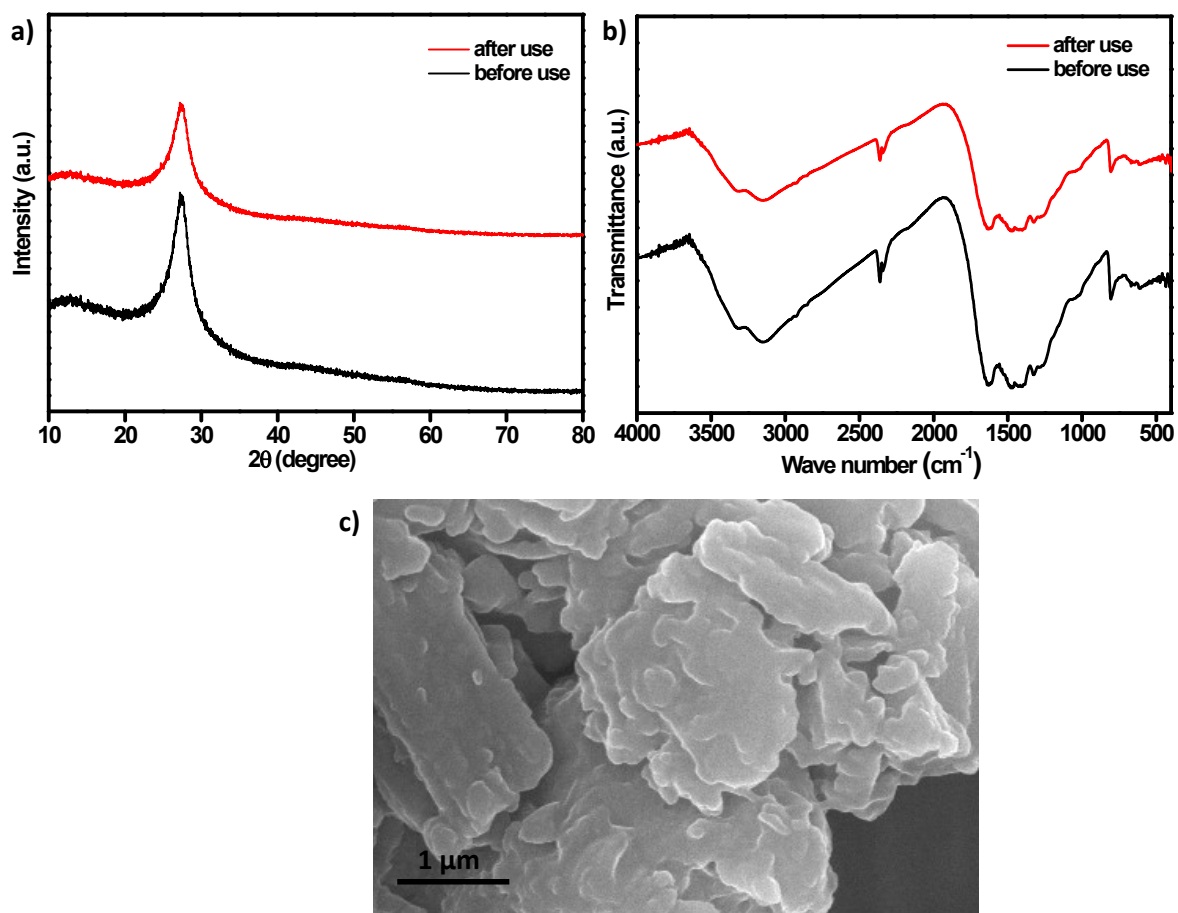


Figure S3 a) PXRD, b) FTIR, c) FESEM images of e-BCN after photocatalytic reactions.

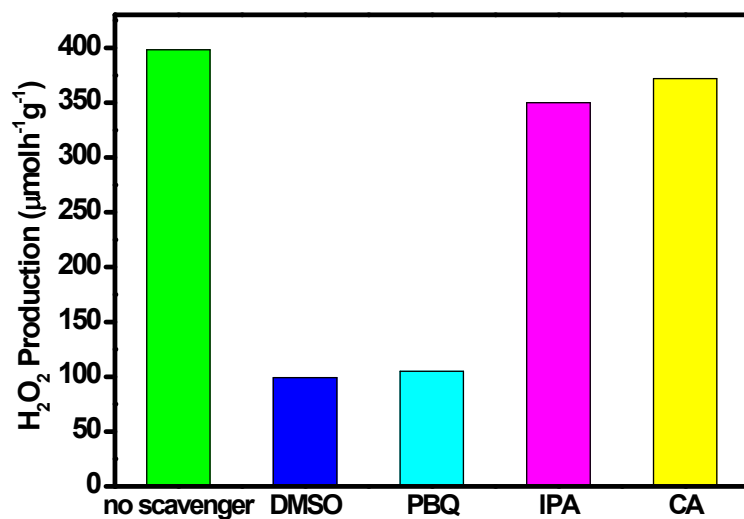


Figure S4 Role of scavenging agents toward photocatalytic H₂O₂ production.

Table S1 Photocatalytic H₂O₂ production and H₂ evolution for other reported g-C₃N₄ based samples under light irradiation

Sl. No.	Photocatalyst	Light source	Photocatalytic performance	Reference
Photocatalytic H ₂ O ₂ production				

1	Na-doped g-C ₃ N ₄	300 W Xe lamp	16.05 mM h ⁻¹	1
2	Na/K doped g-C ₃ N ₄ with N vacancy	300 W Xe lamp	10.2 mM h ⁻¹ g ⁻¹	2
3	g-C ₃ N ₄ with N vacancy	300 W Xe lamp	200 μM h ⁻¹	3
4	Ti ₃ C ₂ / g-C ₃ N ₄	300 W Xe lamp	2.20 μM L ⁻¹	4
5	C, O-doped g-C ₃ N ₄	300 W Xe lamp	60 μM (in 30 h)	5
6	This work	250 W Xe lamp	398.3 μmol h ⁻¹ g ⁻¹	
Photocatalytic H ₂ evolution				
7	P-CN	300 W Xe lamp	1400 μmol h ⁻¹ g ⁻¹	6
8	C-doped CN	300 W Xe lamp	1224 μmol h ⁻¹ g ⁻¹	7
9	P-doped CN	300 W Xe lamp	916.2 μmol h ⁻¹ g ⁻¹	8
10	amino-functionalized ultrathin nanoporous boron-doped g-C ₃ N ₄	300 W Xe lamp	3800 μmol h ⁻¹ g ⁻¹	9
11	0.15-NVCN@Pt	300 W Xe lamp	99.4 μmol h ⁻¹	10
12	This work	150 W Xe lamp	1985 μmol h ⁻¹ g ⁻¹	

3. Reference

1. L. Chen, C. Chen, Z. Yang, S. Li, C. Chu and B. Chen, *Adv. Funct. Mater.*, 2021, **31**, 2105731.
2. S. Wu, H. Yu, S. Chen and X. Quan, *ACS Catal.*, 2020, **10**, 14380-14389.
3. H. Fattahimoghaddam, T. Mahvelati-Shamsabadi and B.-K. Lee, *ACS Sustain. Chem. Eng.*, 2021, **9**, 4520-4530.
4. Y. Yang, Z. Zeng, G. Zeng, D. Huang, R. Xiao, C. Zhang, C. Zhou, W. Xiong, W. Wang, M. Cheng, and W. Xue, *Appl. Catal. B: Environ.*, 2019, **258**, p.117956.
5. S. Samanta, R. Yadav, A. Kumar, A.K. Sinha, and R. Srivastava, *Appl. Catal. B: Environ.*, 2019, **259**, p.118054.
6. C. Han, P. Su, B. Tan, X. Ma, H. Lv, C. Huang, P. Wang, Z. Tong, G. Li, Y. Huang, and Z. Liu, *J. Colloid and Interface Sci.*, 2021, **581**, pp.159-166.
7. E. Liu, X. Lin, Y. Hong, L. Yang, B. Luo, W. Shi, and J. Shi, *Renew. Energ.*, 2021, **178**, pp.757-765.
8. B. Wang, H. Cai, D. Zhao, M. Song, P. Guo, S. Shen, D. Li, and S. Yang, *Appl. Catal. B: Environ.*, 2019, **244**, pp.486-493.
9. M.K. Hussien, A. Sabbah, M. Qorbani, M.H. Elsayed, P. Raghunath, T.Y. Lin, S. Quadir, H.Y. Wang, H.L. Wu, D.L.M. Tzou, and M.C. Lin, *Chem. Eng. J.*, 2022, **430**, p.132853.

10. K. Huang, C. Li, J. Yang, R. Zheng, W. Wang, and L. Wang, *Appl. Sur. Sci.*, 2022, **581**, p.152298.